



Resilience and ductility of Oxy-fuel HAZ cut

A. Martín-Meizoso, J. Aldazabal, J.L. Pedrejón
CEIT and Tecnun (University of Navarra)
ameizoso@ceit.es

S. Moreno
Tecnun (University of Navarra)
s.moreno@alumni.tecnun.es

ABSTRACT. Cutting processes affect the material to a deeper or shallower attached-to-the-cut zone. Its microstructure, its hardness and mechanical properties are changed. Also the cutting process introduces surface roughness and residual stresses. In most cases it is recommended to remove this region by grinding, in order to keep a smoother surface, free from the above mentioned effects. This work presents the characterization results of the Heat Affected Zone (HAZ) of a steel plate of grade S460M, with a thickness of 25 mm, cut by flame oxy-fuel gas cutting. The HAZ microstructure is observed (and the depth of the HAZ measured), the hardness profile and the stress vs. strain curves until fracture are measured by testing micro-tensile samples, instrumented with strain gauges. Micro-Tensile specimens are 200 microns in thickness and were obtained from layers of the HAZ at different distances from the oxy-fuel cut. The obtained stress-strain curves are compared with the hardness measurements and the observed metallography.

KEYWORDS. Cutting; HAZ; Oxy-fuel; steel; Cut Affected Zone (CAZ).

INTRODUCTION

The use of plates as part of constructions, structures, machinery... requires the cutting of large plates into smaller parts that eventually will be shaped and arranged together by means of mechanical joining techniques or welds. There are many available techniques for cuttings: shear cutting, oxy-fuel gas or flame cut, laser cut, plasma, water jet... all these techniques will affect the cut material to a shallower or deeper extent, modifying its microstructure, surface roughness and finishing and might also introduce residual stresses in the neighbour underlying parent material [1-5]. To optimize the use of cutting, particularly with respect to fatigue performances [6-11], the question of to what extent is a good idea to remove cut affected zones (for example, by grinding -what also introduces additional modifications on cut substrates-) is most relevant.

This is the objective of a European Project (HIPERCUT) what deals with plate cutting techniques, ranging from 8 mm to 25 mm plate thickness and grades between S355M and S890Q. Different cutting techniques are studied: plasma, laser and oxy-fuel gas cuttings within this project. This paper is focused on the results obtained for a single grade (S355M), thickness (25 mm) and cutting technique (oxy-fuel gas).

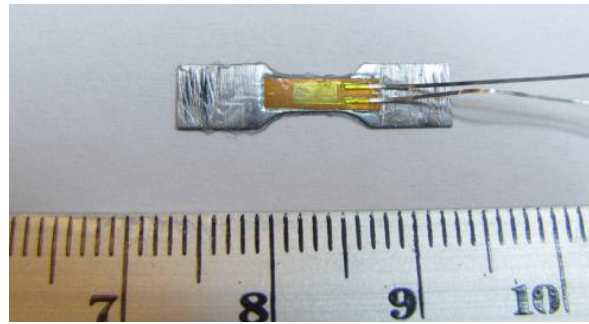


Figure 1: Mini-Tensile testpiece, instrumented with a strain gauge.

MATERIALS AND EXPERIMENTAL TECHNIQUES

This work presents the characterization of a cut edge of a thick (25 mm) plate made of a steel of intermediate strength (S460M). This plate is cut by oxy-fuel gas (flame cut) under the standard industrial cutting conditions typical for heavy plates.

From adjacent-to-the-cut region samples were obtained for metallography, hardness measurements and mini-tensile specimens. Metallographic samples were embedded in a conductive acrylic resin (Condufast). Afterwards the observation side is prepared by polishing with SiC papers until grade 1200 and it is further polished -to a mirror finish- by using velvet clothes with a diamond paste of 6 microns. Finally the samples are etched with 2% nital for 15 s and observed on an optical microscope (Leica MEF-4).

Hardness profiles were carried out with a LECO M-400-G2, equipped with a Vickers' pyramid and using an indentation load of 4.93 N (0.5 kg).

Mini-Tensile probes were cut by Wire Electro-Discharge Machining (WEDM). Twelve prisms -with a dog-bone shape- were machined perpendicular to the cut edge. Four of them were obtained from the upper region of the cut (torch side), four from the middle thickness of the cut, and the other four from the lowest part of cut (flame exit and slag side). The middle sections of mini-tensiles are then located at 2.5 mm from the upper surface, at the middle (12.5 mm) and at 2.5 mm above the lower plate surface.

Afterwards, these prisms are sliced into 300 microns sheets. These sheets are displaced by 150 microns among the different prisms, thus mini-tensiles are distributed with a resolution of 150 microns in distance from cut surface. Mini-tensiles are extracted with a longitudinal orientation (L) with respect to the plate rolling direction and their surfaces parallel to cut edge.

According to literature [12-13], WEDM introduces residual stresses and affects to a depth of about 80 microns. In order to remove the effects of WEDM, 50 microns from each side of the test-piece are grinded away and the samples are then polished with SiC 1200 grade paper and velvet cloth with diamond paste of 6 microns. Test-pieces are not moved during polishing (at the automatic polishing machine: Struers) to provide a longitudinal polishing pattern, parallel to the future loading direction. The final test-piece thickness is 200 microns (nominally. It will be measured for each individual test-piece). The cut edge surface is not polished, but retained for the most superficial test-piece. This first mini-tensile test-piece is only polished at the inner surface (twice as hard -removing 100 microns for this side- to result in an identical final thickness of approx. 200 microns).

Fig. 1 shows a mini-tensile probe. Its basic dimensions are 20 mm in total length, 5 mm total width, 2.5 mm width in the reduced waist section and 0.2 mm thickness.

To obtain accurate strain measurements, individual test-piece are instrumented with one strain gauge (HBM 1-LY11-3/120 with a 5% of maximum strain). A San-Ei amplifier is used to record strain gauge elongations. Tensile tests are conducted at a ram speed of 0.1 mm/minute. For strains larger than a 5%, the ram position records are used (after correlation with the previous strain measurements obtained from the strain gauge).

An electro-mechanical testing machine (Instron Mini 44) is used to carry out the mini-tensile tests. This testing machine has a load cell of ± 500 N. Test-piece heads are introduced into a slot machined at the ends of two volts. These slots are 300 microns thick. Then test-piece heads are glued in position with cyanoacrylate adhesive (Loctite), capillarity does the filling. Fig. 2 shows the experimental arrangement.

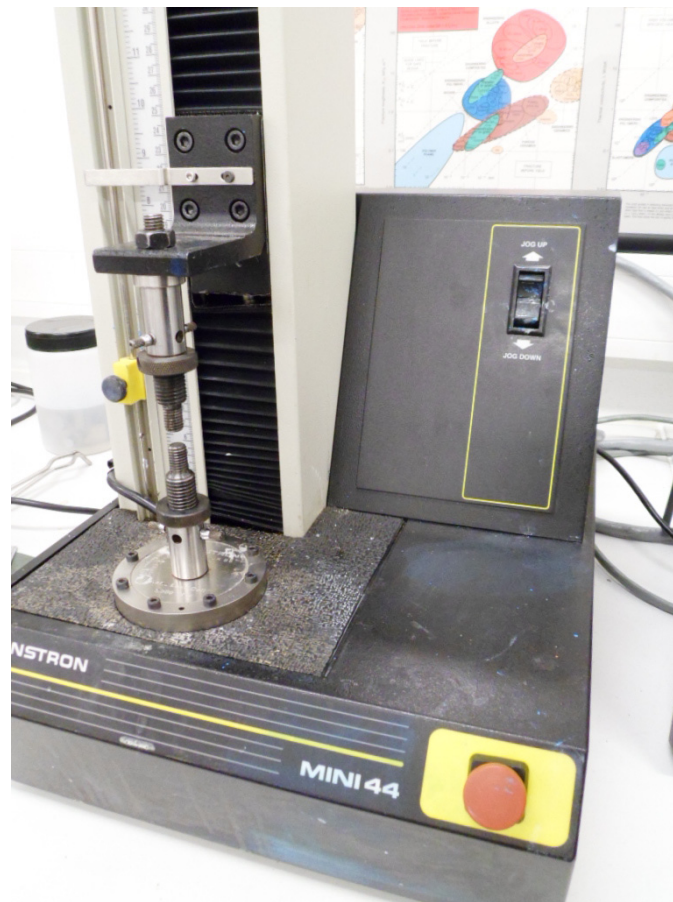


Figure 2: Mini-Tensile experimental arrangement.

RESULTS

Metallography

Figure 3 shows an etched metallographic section through Cut Affected Zone (CAZ). CAZ is much wider at the exit side (slag side) than at the middle or at the top (torch side) of the cut edge thickness. In a similar way to a welding process, the heat generated during cutting and welding produces phase transformation and grain growth of underlying parent material, as it is shown in Fig. 4.

At the region closest to cut edge, martensite and bainite layers are observable. At a distance of 200 microns from cut edge polygonal ferrite is observed. At about 400 microns, ferrite grains are larger and beyond 850 microns pearlite and even larger polygonal ferrite grains are observed; this last microstructure corresponds to unmodified base material (hypoeutectoid steel, with pearlite-ferrite bands).

Microhardness

Fig. 5 shows hardness profiles (Vickers 0.5 kg, HV05) obtained from top (at 0.5 and 2.5 mm from top plate surface), middle and bottom (at 0.5 and 2.5 mm above lower plate surface) of cut edge thickness versus distance from cut edge.

Mini-Tensiles tests

Fig. 6 shows a typical tensile fracture of a mini-tensile probe after necking.

Fig. 7, 8 and 9 summarize the obtained results from tensiles tests. Stress vs. strain is depicted as a function of distance from the oxy-fuel cut, for locations close to the top of the cut (2.5 mm from upper plate surface), middle of the cut edge thickness and close to the bottom (2.5 mm above exit side of slag jet).

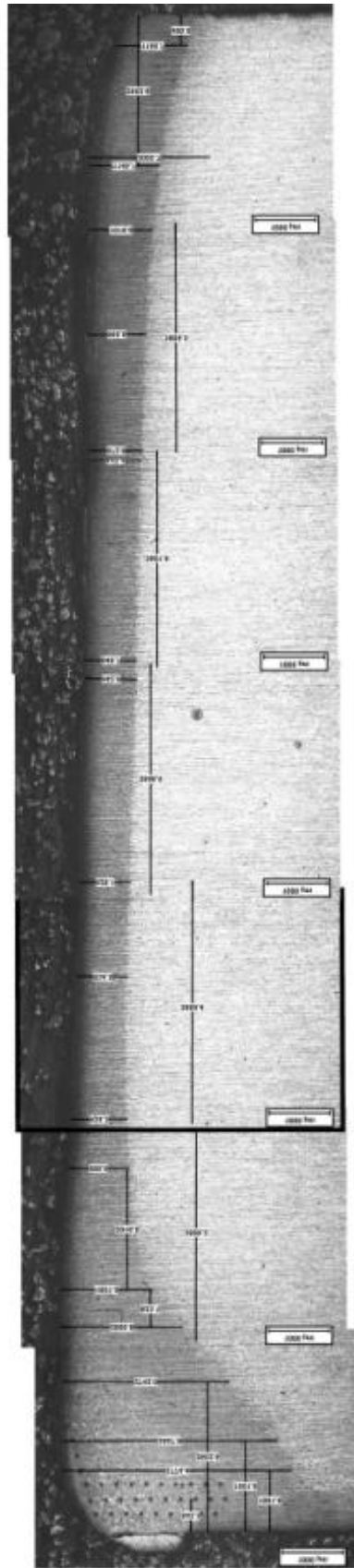


Figure 3: Etched metallographic section, showing oxyfuel Cut-Affected Zone.

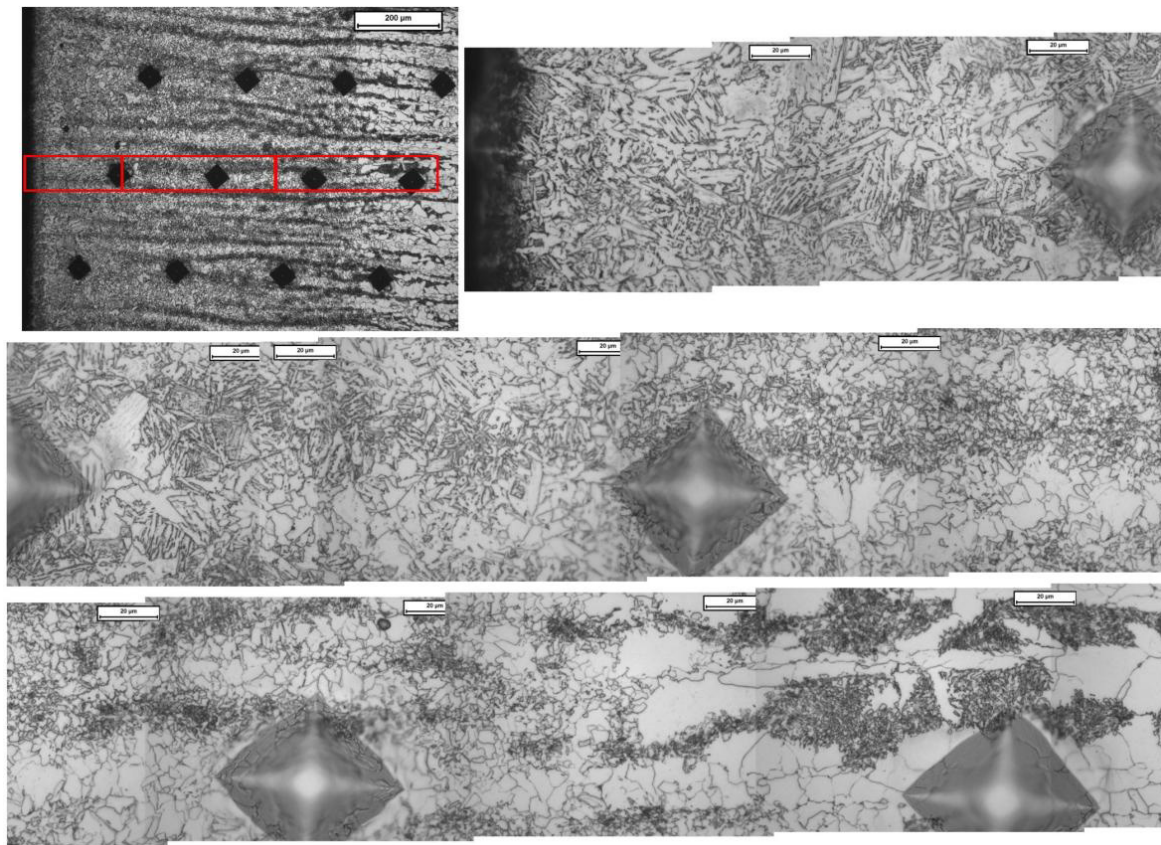


Figure 4: Details of CAZ, at middle thickness of cut edge, showing Vickers' hardness indentations.

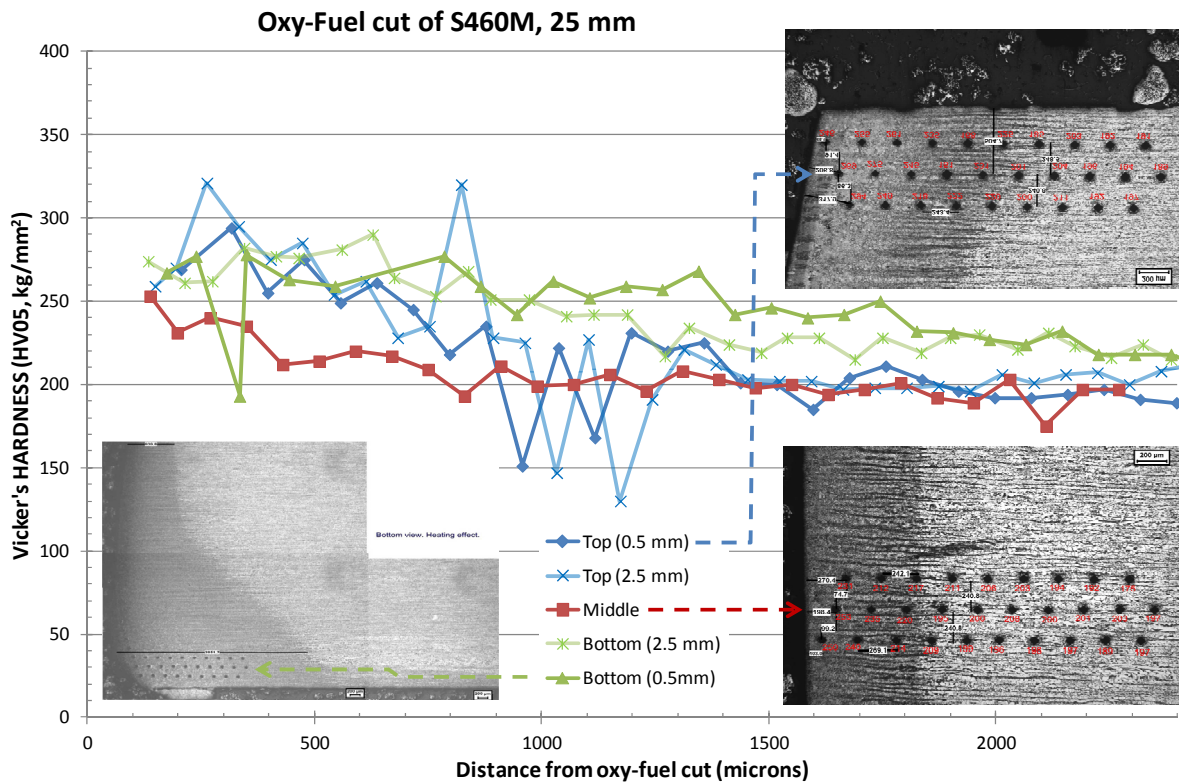


Figure 5: Micro-hardness profiles vs. distance from cut edge.

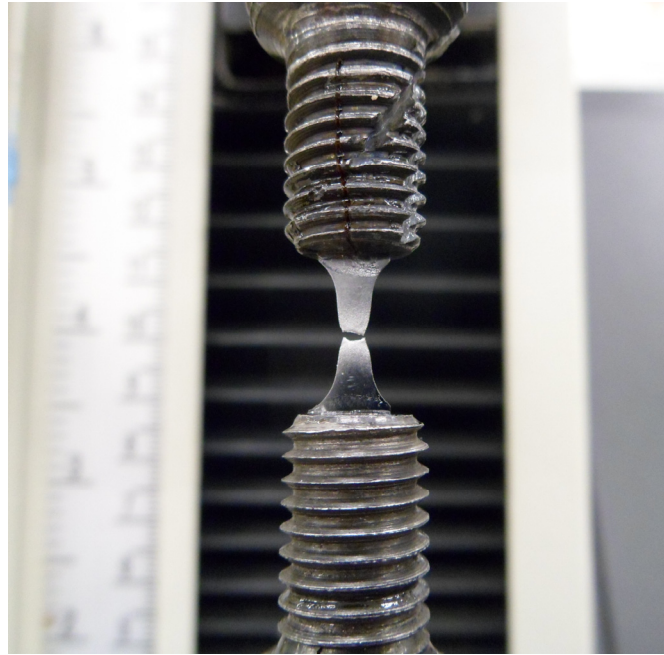


Figure 6: Necking and fracture of a mini-tensile probe.

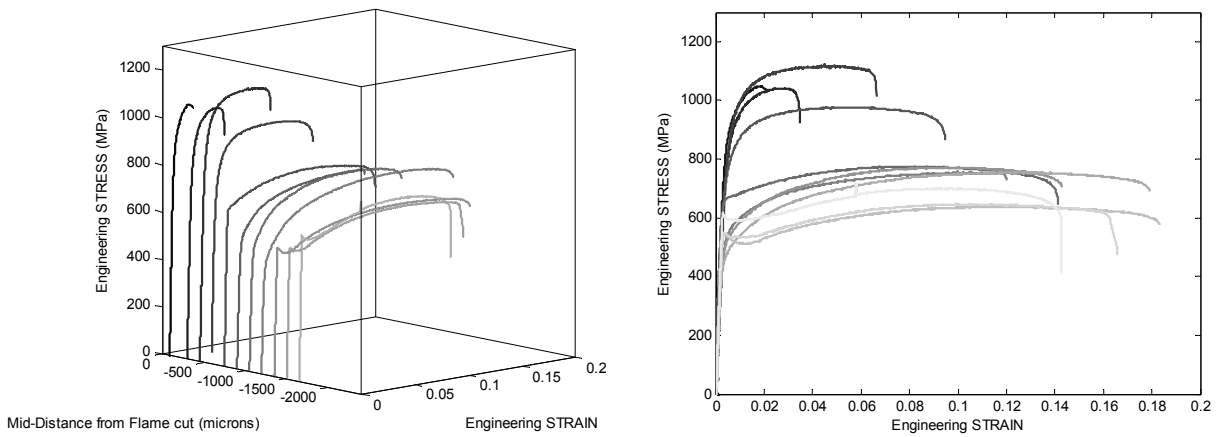


Figure 7: Evolution of engineering stress vs. engineering strain as a function of distance from oxy-fuel cut edge, for the upper locations of cut edge (2.5 mm below upper plate surface).

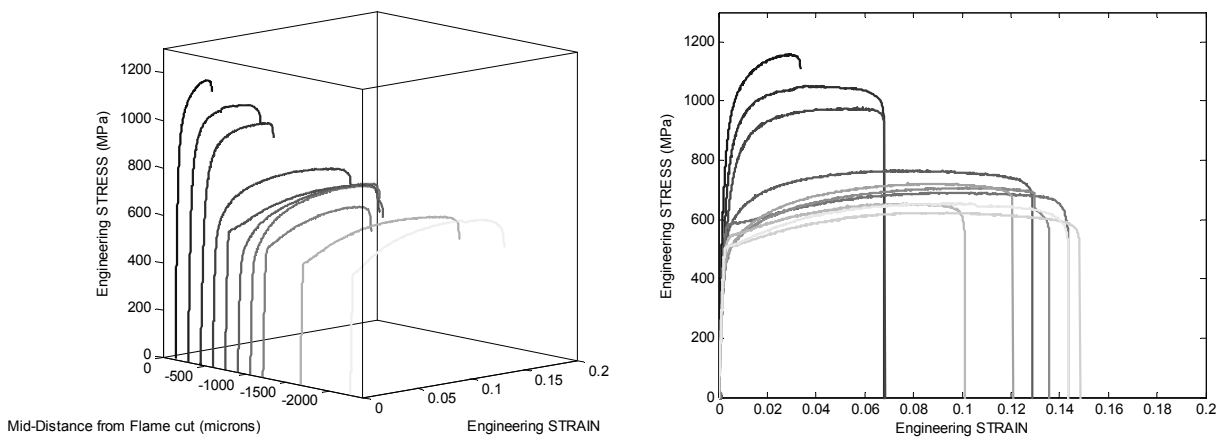


Figure 8: Evolution of engineering stress vs. engineering strain as a function of distance from oxy-fuel cut edge, for middle thickness location of cut edge.

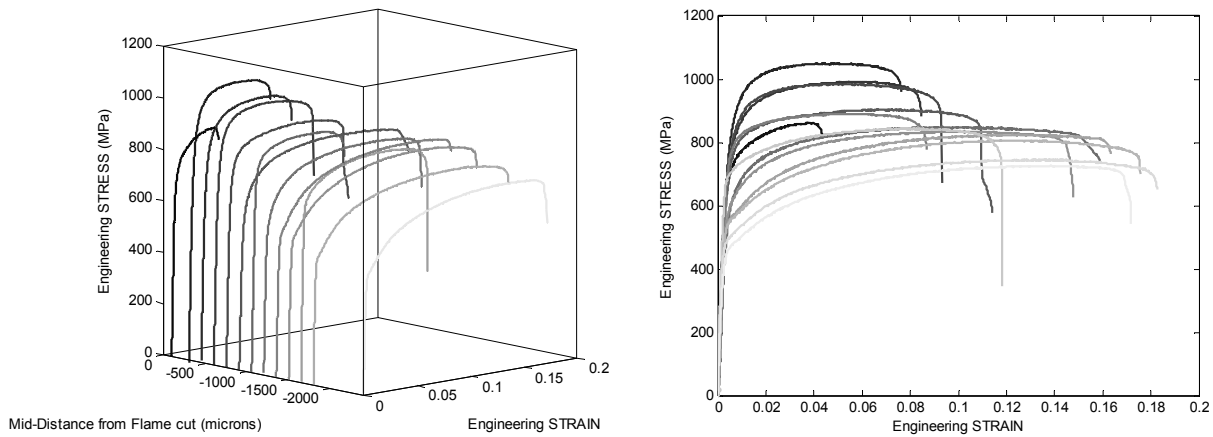


Figure 9: Evolution of engineering stress vs. engineering strain as a function of distance from oxy-fuel cut edge, for middle thickness location of cut edge.

Fig. 10 represents the evolution of mechanical strength parameters (yield stress, ultimate tensile stress...) vs. distance from the oxy-fuel cut, for the middle thickness location.

Fig. 11 shows the evolution of the maximum uniform strain (until necking) and fracture strain vs. distance from the oxy-fuel cut, at the same middle location.

Fig. 12 shows the evolution of the strain hardening index vs. distance from cut, for the three studied locations: 2.5 mm below the top surface, at the middle of the cut edge thickness and 2.5 mm above the exit side.

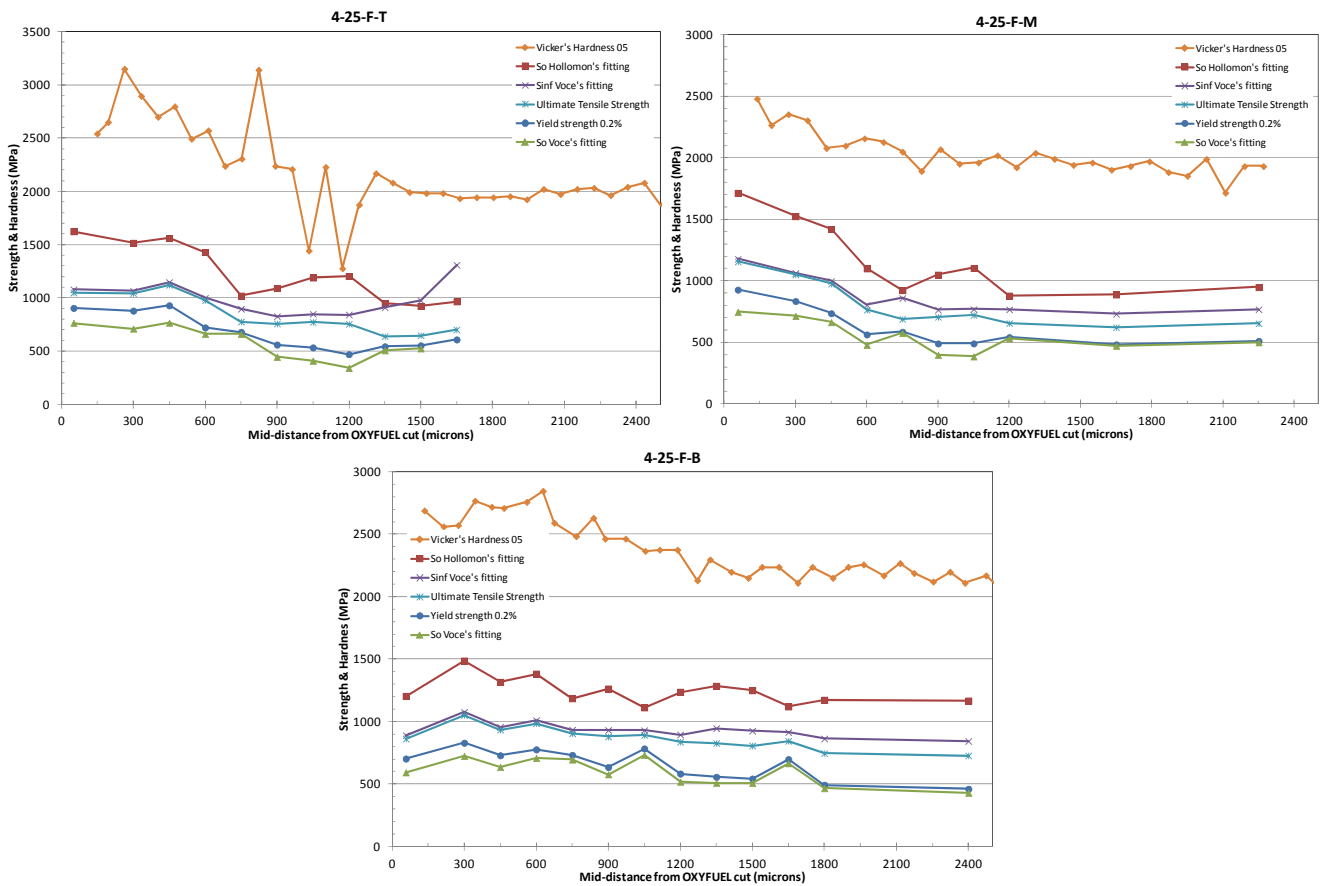


Figure 10: Evolution of Vickers' hardness (converted into MPa units), yield strength, ultimate tensile and other fitting parameters with MPa units, as a function of distance from oxy-fuel cut for the top, middle and bottom positions across the cut edge thickness.

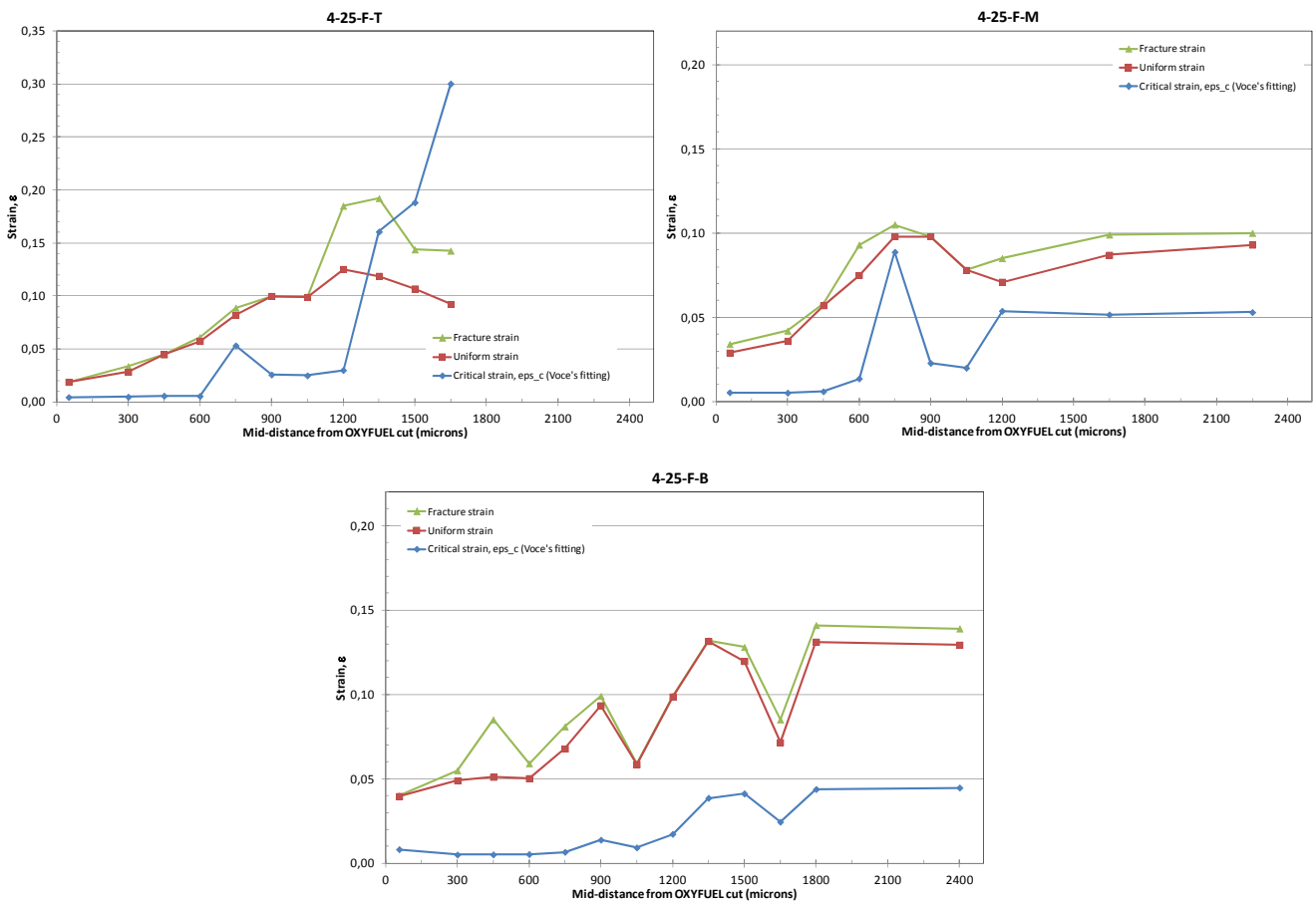


Figure 11: Evolution of uniform strain (necking strain), fracture of maximum strain and critical strain (of Voce's fitting), as a function of distance from oxy-fuel cut for the top, middle and bottom positions across the cut edge thickness.

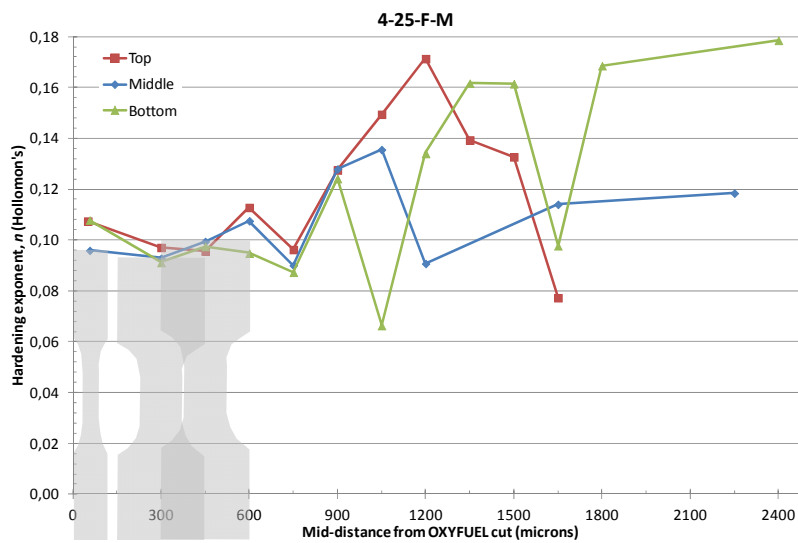


Figure 12: Evolution of strain hardening index (Voce's fitting) as a function of distance from oxy-fuel cut for the top, middle and bottom positions across the cut edge thickness.



CONCLUSIONS

The technical feasibility of obtaining local flow curves (stress vs. strain) of different sheets close to a cut has been probed. It was carried out by means of mini-tensile probes, machined by WEDM, and instrumented with strain gauges. The load carried by the strain gauge was measured (in an independent test) and these –not negligible– loads are subtracted, before further processing of results.

Oxy-fuel heat affected zone is quite thin at the middle of the cut edge thickness (850 microns), a bit larger at the top of the cut and very wide at the jet slag exit side (of about 2 mm). The same results are observed from the metallography and the microhardness measurements.

Measurements of surface roughness and residual stresses vs. depth, by X-ray diffraction, are under completion.

ACKNOWLEDGMENTS

The authors want to thank to the European Union for the financial support of this work, carried out within HIPERCUT project (RFSC-CT-2012-00027).

REFERENCES

- [1] Tomas, D.J., Characterisation of steel cut edges for improved fatigue property data estimations and enhanced CAE durability. Ph.D. Thesis in engineering, Swansea University, UK (2011).
- [2] BS EN ISO 9013: 2002, Thermal Cutting – Classification of thermal cuts – Geometrical products specification and quality tolerances (2004).
- [3] The Steel Construction Institute, Guidance Notes on best practice in steel bridge construction, P185, Fifth issue, Steel Bridge Group (2010).
- [4] Kirkpatrick, I., Variety of cutting processes spoil fabricators for choice, *Welding & Metal Fabrication*, 62 5 (1994) 11-12.
- [5] Avila, M., Which Metal-Cutting Process Is Best for Your Application, *Welding Journal*, (2012) 32-36.
- [6] Goldber, F., Influence of thermal cutting and its quality on the fatigue strength of steel, *Welding Journal*, 52 (9) (1973) 392-404.
- [7] Plecki, R., Yeske, R., Alstetter, C., Lawrence, F.V. Jr., Fatigue resistance of oxygen cut steel. *Welding Journal* 56, 8 (1977) 225-230.
- [8] Ho, N.-J., Lawrence, F.V., Alstetter, C.J., The fatigue resistance of plasma- and oxygen-cut steel, *Welding Research Supplement* (1981) 231-236.
- [9] Piraprez, E., Fatigue strength of flame-cut plates, *Fatigue of Steel and Concrete Structures*, Proc. IABSE Colloquium Lausanne (March 1982) IABSE Reports 37. International Association for Bridge and Structural Engineering, Zurich, Switzerland, (1982) 23-26.
- [10] Wood, W.E., Heat-Affected Zone Studies of Thermally cut Structural Steels, US Department of Transportation Federal Highway Administration Report FHWA-RD-93-O, 15 (1994).
- [11] Kaufmann, I., Schonherr, W., Sonsino, C.M., Fatigue strength of high-strength fine-grained structural steel in the flame cut condition. *Schweissen u. Schneiden*, 3 (1995) E46-E51.
- [12] García Navas, V., Ferreres, I., Marañón, J.A., García-Rosales, C., Gil Sevillano, J., Electro-discharge machining (EDM) versus hard turning and grinding, Comparison of residual stresses and surface integrity generated in AISI O1 tool steel, *J. of Mater. Process. Techn.* (2007).
- [13] García Navas, V., Optimización del procesos de mecanizado mediante control de tensiones residuales y otros parámetros de integridad estructural. Ph.D. Thesis, University of Navarra (2006).